

# DIP Project Report

Ajit Srikanth\*  
IIIT-Hyderabad

ajit.srikanth@research.iiit.ac.in

Jhalak Banzal\*  
IIIT-Hyderabad

jhalak.banzal@students.iiit.ac.in

Sunayana Samavedam  
IIIT-Hyderabad

Anoop Namboodiri  
IIIT-Hyderabad

*\* denotes equal contribution*

## 1 Overview

The primary objective of our project was to implement haze removal using the Dark Channel Prior (DCP) method. However, we not only successfully implemented DCP, but also enhanced its performance slightly. In addition to this, we extended our work by implementing two other notable techniques—one that builds upon DCP and another that serves as a prior work—and conducted a comparative analysis of multiple methods.

To demonstrate the practical significance of these methods, we explored their effectiveness in a downstream task: object detection and tracking. This application highlights the value of improved haze removal in real-world scenarios, such as autonomous driving and surveillance, where clear image quality is crucial for accurate detection and tracking.

In short, below are our completed objectives:

- Implementation of the paper "Single Image Haze Removal Using Dark Channel Prior" from scratch
- Two alternate methods for obtaining speedups in their algorithm.
- Added an additional preprocessing step to improve the restored image quality by utilizing CLAHE
- Implementation of the paper "Single Image Haze Removal Using Color Attenuation Prior" from scratch
- Implementation of the paper "Bayesian Defogging" from scratch
- Comparison of the above algorithms along with some other classical methods such as Magic Light Filter, HBF + power law transforms
- Implemented a pipeline for image dehazing followed by object detection and tracking (using YOLO).

Slides : [Canva Link](#)  
Code : [Drive Link](#)

## 2 Introduction: Haze Removal

Haze and fog significantly degrade the quality of images by reducing contrast, muting colors, and obscuring scene details. These visual impairments hinder crucial applications such as autonomous navigation, object recognition, and environmental scene analysis. The degradation arises from the interaction between light and atmospheric particles. Specifically, light reflected from objects in the scene is attenuated as it travels to the camera, losing intensity based on the scene's depth. Simultaneously, scattered atmospheric light, or airlight, is added to the image, brightening the scene unevenly depending on the density of haze and the distance of objects. This combination fundamentally alters the appearance of the captured image.

Recovering a clear image from a single hazy input is particularly challenging due to the intertwined effects of attenuation and airlight, which depend on the depth of the scene elements relative to the camera. As Narasimhan and Nayar (2002) described, the weather-degraded image is governed by a bilinear relationship between scene albedo (true color and reflectance) and depth. This coupling means the observed image provides incomplete and ambiguous information about these underlying factors. Without explicit depth data or multiple viewpoints, this creates an ill-posed inverse problem—multiple combinations of depth and albedo can explain the same degraded image, making it extremely difficult to accurately restore the true scene appearance.

Traditional methods address these challenges by incorporating external information. Polarization-based techniques use multiple images with varying polarization to separate airlight and scene radiance, while other approaches leverage images captured under different weather conditions to estimate depth. Depth-based methods often require user input or rely on known 3D models to constrain the problem. However, these methods are impractical for single-image scenarios due to their reliance on additional data.

Recent advances have shifted focus to single-image

dehazing methods, which attempt to infer missing information through strong assumptions or priors. For example, Tan’s method enhances local contrast to generate visually appealing results but lacks physical accuracy. Fattal’s method estimates scene albedo and transmission by assuming they are locally uncorrelated, achieving realistic outputs but faltering with dense haze or in cases where the assumption breaks down.

The model widely used to describe the formation of a haze image is:

$$I(x) = J(x)t(x) + A(1 - t(x)), \quad (1)$$

where,

- $I(x)$  is the observed hazy image.
- $J(x)$  is the scene radiance (haze-free image).
- $t(x)$  is the transmission map, representing the portion of light that reaches the camera.
- $A$  is the global atmospheric light.

### 3 Single Image Haze Removal Using Dark Channel Prior

Our primary paper to implement, **Single Image Haze Removal Using Dark Channel Prior** [1] introduces a novel method to remove haze from a single image using the *Dark Channel Prior (DCP)*. The authors propose a simple yet effective prior based on the observation of natural, haze-free outdoor images and develop a haze removal algorithm that significantly enhances image clarity.

#### 3.1 Dark Channel Prior (DCP)

The *Dark Channel Prior* is based on the observation that in most haze-free outdoor images, some local image patches contain pixels with very low intensity in at least one color channel (RGB). These dark pixels result from shadows, colorful objects, or surfaces that absorb light.

Mathematically, the dark channel of an image  $J$  is defined as

$$(J^{dark})(x) = \min_c \left( \min_{y \in \Omega(x)} J^c(y) \right) \quad (2)$$

where,

- $J^c(y)$  is the intensity of the color channel  $c$  (red, green, blue) at pixel  $y$ .
- $\Omega(x)$  is a local patch centered around  $x$ .

#### 3.2 Atmospheric Light Estimation

The dark channel of a haze image serves as a reliable approximation for haze density. To enhance the estimation of atmospheric light, the top 0.1% of the bright-

est pixels in the dark channel are selected, as these pixels indicate areas with significant haze opacity. Among these selected pixels, the one with the highest intensity in the original image is identified as the atmospheric light.

This approach, grounded in the dark channel prior, is more robust than the “brightest pixel” method. We use it to automatically estimate the atmospheric lights for all images shown in the paper

#### 3.3 Transmission Map Estimation

Assuming assume that the transmission in a local patch  $\Omega(x)$  is constant. We denote the patch’s transmission as  $\tilde{t}(x)$ . Taking the min operation in the local patch on the haze imaging equation 1, we get:

$$\min_{y \in \Omega(x)} I^c(y) = \tilde{t}(x) \min_{y \in \Omega(x)} J^c(y) + (1 - \tilde{t}(x))A^c \quad (3)$$

The *min* operation is performed on three color channels independently, and we take the min operation among three color channels on the above equation and obtain

$$\min_c \left( \min_{y \in \Omega(x)} \frac{I^c(y)}{A^c} \right) = \tilde{t}(x) \min_c \left( \min_{y \in \Omega(x)} \frac{J^c(y)}{A^c} \right) + (1 - \tilde{t}(x)) \quad (4)$$

But, according to the dark channel prior, the dark channel  $J^{dark}$  (given in equation 2) of the haze-free radiance  $J$  tends to be zero. Hence,

$$\min_c \left( \min_{y \in \Omega(x)} \frac{J^c(y)}{A^c} \right) = 0$$

as  $A^c$  is always positive.

Therefore, we get

$$\tilde{t}(x) = 1 - \omega \min_{c \in \{r, g, b\}} \left( \min_{y \in \Omega(x)} \frac{I^c(y)}{A^c} \right), \quad (5)$$

where  $\omega$  is the constant parameter introduced so that we can optionally keep a very small amount of haze for the distant objects.

#### 3.4 Transmission Map Refining (Soft Matting)

The haze imaging equation 1 has a similar form with the image matting equation. A transmission map is just an alpha map. Therefore, they apply a soft matting algorithm to refine the transmission. We obtain the refined transmission map  $t$  from the raw transmission map  $\tilde{t}$  using a soft matting technique to preserve image details:

$$\operatorname{argmin}_t t^T \mathbf{L} t + \lambda \|t - \tilde{t}\|^2, \quad (6)$$

where,

- $\mathbf{L}$  is the matting Laplacian matrix.
- $\lambda$  is a regularization parameter.

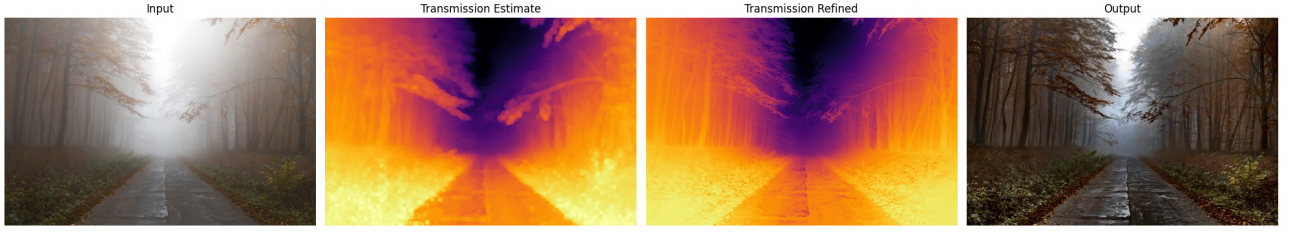


Figure 1: Step by step DCP

### 3.5 Final Scene Radiance Recovery

After obtaining the refined transmission map, the haze-free image is recovered as:

$$J(x) = \frac{I(x) - A}{\max(t(x), t_0)} + A,$$

where  $t_0$  is a lower bound to prevent division by very small values.

### 3.6 Overall DCP Algorithm

1. **Estimating Atmospheric Light( $A$ )** using the **Dark Channel Prior**
2. **Estimating the raw transmission map** from  $A$
3. **Refining the raw transmission map** through soft matting
4. **Recovering the Haze-Free Image** using the obtained  $t(x)$  and  $A$ .

### 3.7 Strengths

The Dark Channel Prior has been widely appreciated for its simplicity and effectiveness in handling single image dehazing. Some notable strengths include:

1. **High-Quality Results:** The method consistently achieves visually pleasing dehazing effects, restoring sharpness and contrast in diverse real-world images.
2. **Wide Applicability:** DCP works effectively across various types of hazy images

### 3.8 Limitations

While DCP has been revolutionary in image dehazing, it still has a few limitations:

1. **Invalid Assumptions in some Bright Scenes:** The core assumption of the dark channel being nearly zero in non-sky regions breaks down in scenes dominated by bright or white regions, such as snow-covered landscapes or overexposed images. In such cases, DCP may fail to produce accurate transmission maps.
2. **Halo Artifacts:** The method is prone to generating halo artifacts, particularly around strong edges or in areas with abrupt changes in depth, such as object boundaries.

3. **High Computational Cost:** Although the principle is simple, refining the transmission map often involves computationally expensive operations like soft matting, limiting the method’s feasibility for real-time applications.

4. **Parameter Sensitivity:** The patch size  $\Omega(x)$  parameters and Soft Matting parameters must be carefully tuned for different images to get optimal results.

## 4 Improving DCP

While DCP can improve visibility by making foggy regions more transparent, it often results in **homogenized or flat colors**. This happens because DCP applies a global enhancement to the image, leading to areas with similar intensity or color being treated uniformly.

For example, in areas like the sky, roads, or distant objects, the natural variation in color or texture is flattened, as DCP doesn’t differentiate much between subtle tonal variations in these regions. As a result, the image can lose its color depth and appear washed out or overly smooth.

Moreover, it often sacrifices fine details and textural contrast. This happens because it focuses on global contrast adjustment rather than preserving local image details. In scenes with complex or fine textures—such as foliage or detailed surfaces—DCP may fail to preserve those subtleties. For instance, if a region has intricate texture in the shadows or midtones, DCP’s broad, uniform adjustment can blur those details, making the image appear flatter and less dynamic.

### 4.1 Contrast Limited Adaptive Histogram Equalization

We propose to improve DCP by incorporating Contrast Limited Adaptive Histogram Equalization (CLAHE) as a pre-processing step. CLAHE is a variant of Adaptive Histogram Equalisation (AHE), where the contrasts of the local patches are clipped. We find that integrating CLAHE with DCP greatly improves the image reconstruction, reduces some artifacts and parameter tuning, required to get a better output, by a reasonable extent.

CLAHE adjusts the contrast of an image by equalizing histograms within small regions, as follows:

1. **Histogram Calculation:**

$$H(i) = \text{Number of pixels with intensity } i$$

where  $H(i)$  is the histogram value for intensity level  $i$ .

2. **Clipping:** If  $H(i) > \text{clip limit}$ , then:

$$H'(i) = \text{clip limit}$$

where  $H'(i)$  is the clipped histogram value.

3. **Redistribution:** The excess pixels from clipping are redistributed to other bins in the histogram.

4. **Cumulative Distribution Function (CDF):**

$$CDF(i) = \sum_{j=0}^i H'(j)$$

5. **Normalization and Mapping:** The CDF is normalized to map pixel values:

$$S(i) = \text{round} \left( \frac{CDF(i) - CDF_{\min}}{M \times N - CDF_{\min}} \times (L - 1) \right)$$

where  $M$  and  $N$  are the dimensions of the tile, and  $L$  is the number of intensity levels.

6. **Output Image Reconstruction:** Each pixel in the output image is updated based on its corresponding CDF value from its tile.

By combining CLAHE with DCP, the image benefits from both local adjustments (from CLAHE) and global contrast enhancement (from DCP). This allows for better retention of local details and textures that DCP alone might have smoothed out. Thus, the colors remain balanced because the local contrast enhancement helps highlight textures and variations in color while avoiding over-enhancement in the overall image.

For instance, in the image of the cityscape, DCP might make the buildings and sky look flat, while CLAHE restores the vibrancy of the sky and the definition of the buildings, preserving the natural look of the image.

## 4.2 Faster Soft Matting

The main computational bottleneck which affects the speed of our algorithm is the Soft Matting process. To address this, we experiment by replacing traditional soft matting method (Levin's soft matting method) with a faster matting based on the Fast Kernel Laplacian and also using a guided filter for soft matting. The cost function for matting is defined as:

$$E(t) = \sum_i (t_i - \hat{t}_i)^2 + \lambda \sum_{ij} w_{ij} (t_i - t_j)^2, \quad (7)$$

where,

- $\hat{t}_i$ : Initial transmission estimate for pixel  $i$ .

- $t_i$ : Refined transmission for pixel  $i$ .
- $w_{ij}$ : Weight function based on the pixel similarity in a local patch.
- $\lambda$ : Regularization parameter.

The Fast Kernel Laplacian simplifies the computation of  $\sum_{ij} w_{ij} (t_i - t_j)^2$  using efficient filtering techniques, drastically reducing the computational complexity. This refinement maintains the accuracy of the transmission map while achieving significant speed-up of **upto 4.6 times**- from **12.4s** to **2.7s**.

Further, we can also use a guided filter for soft matting, which reduces the  $O(n^3)$  time complexity (of Levin's soft matting method) to  $O(n)$  time complexity, at the cost of some performance or mat accuracy. Making the algorithm even faster at around **1.1s**.

Using the guided filter for soft matting is as follows:

1. **Obtain a Coarse Transmission Map:** Start with an initial estimate of the transmission map, which can be derived from techniques like dark channel prior or other matting methods.
2. **Select the Guidance Image:** The guidance image can be the original input image or a different image that provides useful structural information. This choice helps in preserving edges and details during filtering.
3. **Define Parameters:** Set the **window radius**  $r$  and the **regularization parameter**  $\epsilon$ . The window radius determines how much local context is considered during filtering, while  $\epsilon$  controls the degree of smoothing applied.
4. **Apply the Guided Filter:** The guided filter operates by modeling the output as a linear transformation of the guidance image within local windows. For each pixel, it computes:

$$q_i = a_k I_i + b_k$$

where  $q_i$  is the output at pixel  $i$ ,  $I_i$  is the pixel value in the guidance image, and  $(a_k, b_k)$  are coefficients determined locally.

This filtering process preserves edges while smoothing out noise or irrelevant details in flat regions.

5. **Output Refinement:** The result is a refined transmission map that retains important structural information from the guidance image, allowing for better alpha matte estimation compared to traditional soft matting methods.

## 5 Colour Attenuation Prior

We further implement **Single Image Haze Removal Using Color Attenuation Prior** [3] which proposes a haze removal algorithm based on the *Color Attenuation Prior (CAP)*. This prior leverages a statistical relationship between the scene depth and the difference in the brightness and saturation of pixels in a hazy image. They formulate a linear model for modeling the

scene depth of the hazy image based on CAP and learn the parameters of the model with a supervised learning method, achieving superior performance with efficient computation. Their Key contributions are as follows:

### 5.1 Color Attenuation Prior (CAP)

The authors observe that in hazy images, scene depth correlates with the pixel brightness and saturation. Specifically:

- In hazy regions, brightness tends to increase while saturation decreases.
- This observation serves as the foundation for the proposed *Color Attenuation Prior*.

They construct a linear model to estimate the depth of the scene based on this prior.

### 5.2 Scene Depth Estimation

The depth map is formulated as a linear model:

$$z = \theta_1 l + \theta_2 s + \theta_3,$$

where,

- $z$  is the scene depth.
- $l$  is the brightness of a pixel.
- $s$  is the saturation of the corresponding pixel.
- $\theta_1$ ,  $\theta_2$ , and  $\theta_3$  are parameters learned through supervised regression.

### 5.3 Efficient Haze Removal

Once the transmission map  $t(x)$  and atmospheric light  $A$  are estimated, the haze-free image is reconstructed as:

$$J(x) = \frac{I(x) - A}{t(x)} + A.$$

### 5.4 Overall Method

#### 1. Feature Extraction for Depth Map:

- Extract brightness ( $l$ ) and saturation ( $s$ ) features from the input hazy image.

#### 2. Supervised Learning for Depth Estimation:

- Use a training dataset of hazy images with corresponding depth maps.
- Learn the parameters  $\theta_1$ ,  $\theta_2$ , and  $\theta_3$  through regression.

#### 3. Transmission Map and Atmospheric Light Estimation:

- Compute the transmission map  $t(x)$  using the estimated depth map  $z(x)$ .
- Estimate atmospheric light  $A$  based on the brightest pixels in the input image.

#### 4. Haze-Free Image Recovery:

- Reconstruct the haze-free image using the haze imaging model.

### 5.5 Strengths

- The algorithm is computationally more efficient than DCP
- The learning-based approach enables robust depth estimation across various scenes.
- Superior performance compared to traditional priors like the Dark Channel Prior in certain challenging scenarios.

### 5.6 Limitations

- The method relies on a supervised learning framework, requiring a training dataset with depth annotations.
- May struggle with images where the brightness-saturation relationship does not align with the learned model.

This method effectively combines statistical observation and machine learning to achieve high-quality haze removal while maintaining computational efficiency.

## 6 Bayesian Defogging

Another important baseline we implement is **Bayesian Defogging** [2] as it serves as a sufficient baseline in between basic filtering methods like Homomorphic filtering and more statistical methods like Dark Channel Prior and Color Attenuation Prior. The core idea behind Bayesian defogging is to model the formation of foggy images as a combination of two statistically independent latent variables: albedo and depth.

The inference process involves estimating the posterior distribution of the albedo and depth given the observed foggy image. This is done using Bayes' theorem:

$$P(\text{Albedo}, \text{Depth} | I) \propto P(I | \text{Albedo}, \text{Depth}) P(\text{Albedo}) P(\text{Depth}) \quad (8)$$

Here:

- $P(I | \text{Albedo}, \text{Depth})$  is the likelihood of observing the foggy image given specific values for albedo and depth.
- $P(\text{Albedo})$  and  $P(\text{Depth})$  are prior distributions that encode our beliefs about what values these variables might take before observing the data.

This is represented using a Factorial Markov Random Field (FMRF), which will represent the relationship between observed foggy images and latent variables (albedo and depth) and serve as our energy function. We then utilize a non-linear solver and opti-



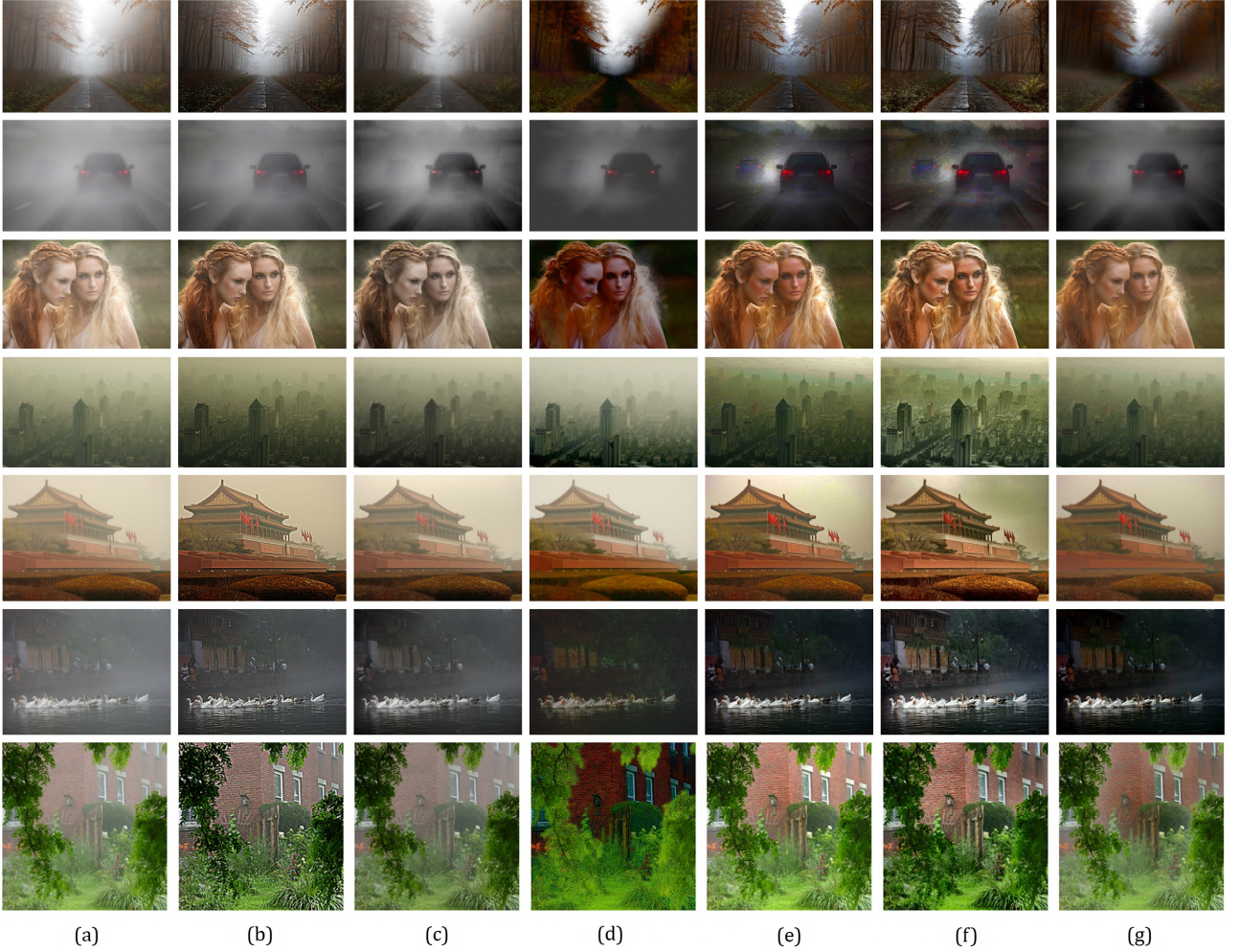


Figure 2: In order: (a) original, (b) HBF + Power law, (c) Homomorphic (magic light) filter, (d) Bayesian Defogging [2], (e) Dark Channel Prior [1], (f) CLAHE + DCP (ours), (g) Colour Attenuation Prior [3]

mize the energy function iteratively until convergence is achieved.

## 7 Comparisons

Apart from the above mentioned methods, we implement two other traditional baselines utilized for image dehazing: **Magic Light (homomorphic) filters**, and **High Boost Filter + Power-Law transform**.

The comparison of dehazing techniques in figure 2 reveals distinct strengths and weaknesses for each method. The original hazy images (a) serve as a baseline, showing poor visibility, low contrast, and degraded colors due to atmospheric scattering and attenuation. The HBF + Power Law method (b) moderately enhances contrast and brightness but often overexposes brighter regions and fails to restore color fidelity completely. The Homomorphic (Magic Light) Filter (c) improves contrast and sharpness effectively, though it tends to over-enhance textures, leading to reduced realism in certain areas.

Bayesian Defogging (d) provides better haze removal and improved color restoration but occasionally introduces artifacts in dense haze regions and is computa-

tionally demanding. The Dark Channel Prior (DCP) (e) achieves significant haze removal and natural color restoration, particularly in outdoor scenes, but suffers from halo artifacts around strong edges and struggles with bright sky regions.

The proposed CLAHE + DCP method (f) addresses these limitations by enhancing visibility and contrast while preserving natural color balance and reducing halo artifacts, making it particularly effective in dense haze conditions. However, in most cases the Color Attenuation Prior (CAP) (g) performed the best, leveraging scene depth for haze removal, but occasionally oversaturates colors and is less effective in extreme haze scenarios.

Overall, the proposed CLAHE + DCP method provides a balanced approach with good performance for certain difficult scenes, while the CAP method provided consistent performance for most general cases, making it a robust choice for practical applications.

## 8 Practical Uses

One of the most critical applications of image dehazing is in autonomous driving, where object detection and

tracking in adverse weather conditions—such as fog or haze—are essential for safety. In such conditions, effective dehazing algorithms are necessary to ensure clear visibility and accurate perception of the environment.

For instance, before dehazing, a vehicle in the left lane might be obscured, posing a potential hazard if the Autonomous Driving Assistance System (ADAS) attempts to change lanes. While the system could still detect and avoid the vehicle at close range, relying on such reactive detection is inherently risky. Thus, efficient dehazing not only improves the performance of ADAS systems but also plays a vital role in preventing accidents and ensuring safer driving in challenging environmental conditions.



Figure 3: Object detection Before and After Dehazing



Figure 4: Enhancements to prevent (not-guaranteed) dying in souls-like games due to poor vision

## 9 References

- [1] Kaiming He, Jian Sun and Xiaoou Tang, "Single image haze removal using dark channel prior," 2009 IEEE Conference on Computer Vision and Pattern Recognition, Miami, FL, USA, 2009, pp. 1956-1963, doi: 10.1109/CVPR.2009.5206515.
- [2] Ko Nishino, Louis Kratz, and Stephen Lombardi. 2012. Bayesian Defogging. *Int. J. Comput. Vision* 98, 3 (July 2012), 263–278, doi: 10.1007/s11263-011-0508-1.
- [3] Q. Zhu, J. Mai and L. Shao, "A Fast Single Image Haze Removal Algorithm Using Color Attenuation Prior," in *IEEE Transactions on Image Processing*, vol. 24, no. 11, pp. 3522-3533, Nov. 2015, doi: 10.1109/TIP.2015.2446191.
- [4] A. Levin, D. Lischinski and Y. Weiss, "A Closed-Form Solution to Natural Image Matting," in *IEEE Transactions on Pattern Analysis and Machine Intelligence*, vol. 30, no. 2, pp. 228-242, Feb. 2008, doi: 10.1109/TPAMI.2007.1177.
- [5] K. He, J. Sun and X. Tang, "Fast matting using large kernel matting Laplacian matrices," 2010 IEEE Computer Society Conference on Computer Vision and

Pattern Recognition, San Francisco, CA, USA, 2010, pp. 2165-2172, doi: 10.1109/CVPR.2010.5539896.

- [6] K. He, J. Sun and X. Tang, "Guided Image Filtering," in *IEEE Transactions on Pattern Analysis and Machine Intelligence*, vol. 35, no. 6, pp. 1397-1409, June 2013, doi: 10.1109/TPAMI.2012.213.